Mitt. naturwiss. Ver. Steiermark	Band 124	S. 29–39	Graz 1994

Some Calculated Thermodynamic Pseudosections from the Plattengneis and Other Rocks of the Koralm Complex, Eastern Alps

Von Kurt STÜWE

Mit 2 Abbildungen und 1 Tabelle

Angenommen am 22. Februar 1994

Abstract: Thermodynamic pseudosections appropriate to four pelitic bulk compositions typical of rock types from the Koralm Complex, Eastern Alps are calculated in the model system K_2O-FeO-MgO-Al_2O_3-SiO_2-H_2O (KFMASH). An average of these four bulk composition has recently been used by STÜWE and POWELL 1994 to discuss the portraying of modal information on thermodynamic pseudosections and its use for the derivation of a *PT* path for the Koralm complex. Here, the individual pseudosections for all samples are presented as a graphical database for this accompanying contribution. In particular, pseudosections are calculated for two *Plattengneis* samples from one of the eastern-most and one of the western-most exposures respectively, one sample from the *Paramorphoseschiefer* and one sample from the *Zentrale Gneis komplex*. These bulk compositions are typical for many pelitic rocks of the Austroalpine and the pseudosections presented here should therefore provide a simple tool for the interpretation of many metamorphic rocks. For the Koralm complex, the pseudosections indicate principal formation conditions of at least 14 kbar and probably around 700°C, but they indicate a high pressure pre-history for some samples. The retrograde evolution of at least the Plattengneis samples appears to be characterised by initial isobaric cooling after the peak.

Zusammenfassung: In diesem Artikel werden vier thermodynamische Pseudoschnitte vorgestellt, die für verschiedene pelitische Gesteinszusammensetzungen von Gesteinen aus dem Koralmkristallin berechnet wurden. Die Pseudoschnitte wurden im Sechskomponentensystem K_2O-FeO-MgO-Al_2O_3-SiO_2-H_2O (KFMASH) berechnet. Eine mittlere Gesamtgesteinszusammensetzung der hier vorgestellten Proben wurde kürzlich von STÜWE und POWELL 1994 verwendet, um die Darstellung von modalem Mineralbestand auf Pseudoschnitten zu diskutieren und davon einen Druck-Temperatur- (*PT*-)Pfad für die Koralmgesteine abzuleiten. Hier werden die einzelnen Pseudoschnitte aller analysierten Gesteine vorgestellt, und der vorliegende Artikel will daher als die Datenbasis zu der Parallelpublikation von STÜWE und POWELL 1994 verstanden werden. Im einzelnen handelt es sich bei den vier behandelten Proben um zwei Proben aus dem *Plattengneis* (eine von einem der östlichsten Aufschlüsse nahe des Steirischen Beckens und eine von einem der westlichsten Aufschlüsse nahe des Krakaberges), eine Probe von den *Paramorphoseschiefern* sowie eine Probe aus dem *zentralen Gneiskomplex*. Die Gesamtgesteinszusammensetzungen der vier Proben sind typisch für viele Proben aus anderen Bereichen des austroalpinen Deckenstapels, und die hier vorgestellten Pseudoschnitte sollten daher als ein Mittel zur Interpretation vieler Gesteine der Ostalpen dienen. Für den Koralmkomplex deuten die Pseudoschnitte Formationsbedingungen von mindestens 14 kbar und 700°C an, lassen aber ebenso erkennen, daß zumindest manche Gesteine eine Hochdruckvorgeschichte gehabt haben. Die retrograde Geschichte der Gesteine scheint, zumindest beim Plattengneis, mit einem Abkühlen bei konstantem Druck begonnen zu haben.

1. Introduction

Thermodynamic pseudosections of full petrogenetic grids are one of the most useful graphic tools for the interpretation of the formation conditions of metamorphic rocks because: 1. they are much more simple to read than their full grid equivalents as they exclude all reaction information that is irrelevant to the rock of interest; 2. they

can show the boundaries of fields of higher thermodynamic variance and can therefore be used to infer formation conditions of rocks in regions of pressure-temperature (*PT*) space that are *not* crossed by univariant reactions and 3. they can be used to portray other information, for example, compositional information of individual minerals (thermo-barometry) or reaction progress information as evidenced by modal proportions of minerals in the rock. Especially the reaction progress information has been of some interest in the past (e.g. THOMPSON et al., 1982; CHAMBERLAIN, 1986; SCHNEIDERMANN, 1992) as it requires only data that can be obtained by point counting and does therefore not rely on microprobe analysis to infer *PT* paths of rocks of known bulk composition. STÜWE and POWELL 1994 have implemented this information into the software package THERMOCALC of POWELL and HOLLAND 1989 and discussed this method in some detail. They used pseudosections contoured for modal mineral abundances to derive a *PT* path for the Koralm complex from di-, tri- and quadrivariant pelitic assemblages. Because of the focus of their paper on the methodology, they refrained from discussing details of bulk compositions of individual rocks and used only one representative pseudosection to present modal information. They did not discuss pseudosections for specific bulk compositions of individual rocks, nor did they discuss details of the petrography and location of individual samples. This paper presents those details of the individual samples and, importantly, the full information of pseudosections for four specific bulk compositions of typical pelitic gneisses of the Koralm complex. This paper is therefore to be considered as a "data base" to the accompanying contribution of STÜWE and POWELL 1994.

2. Samples and Petrography

The samples collected for this study were collected within part of a multiyear project of Adelaide University on Eastern Alpine tectonics. The particular relevance of the Koralm Complex within this project lies in its high Eoalpine grade. Estimates of the heat budget during Eoalpine metamorphism indicated that there is some problems and inconsistencies with some interpretations of the Cretaceous and Tertiary evolution of the high grade regions on the Eastern Alps. These regions are in particular the Koralm complex in the east as well as the Ötztal complex in the west. Details of the problems arising from such heat budget estimates are discussed elsewhere and form not part of the scope of this paper (see STÜWE, 1991; EHLERS et al., 1994; STÜWE and SANDIFORD, 1994; STÜWE and POWELL, 1994; STÜWE and EHLERS, 1994). Similarily, the regional geology of the Koralm complex will not be repeated here and the reader is referred to the extensive body of previous work (amongst others: HERITSCH, 1978; BECK-MANAGETTA, 1980a, b; MORAUF, 1982; FRANK et al., 1983; KLEINSCHMIDT et al., 1984; KROHE, 1987; MILLER, 1990; THÖNI and JAGOUTZ, 1992). Within a mapping and sampling program for this study 200 samples were collected in the Koralm and Gleinalm region with most samples being collected between Weinebene and Soboth roads to the north and south and the Steirischen Basin and the Lavant valley to the east and west. Of these samples about 100 thin sections were cut. For the study of bulk compositions six samples were selected for analysis. Two of these samples are eclogites which were collected along the Soboth road near the Soboth Dam (sample 51/92) and on the west slope of the Koralm near the Sonnhof (sample 31/92). This paper considers only the other four samples which are of pelitic bulk composition. In the selection of these four samples care was taken to exclude samples containing plagioclase, so that the influence of CaO and Na_2O may be neglected and the samples may be discussed within the model system K_2O-FeO-MgO-Al_2O_3-SiO_2-H_2O (KFMASH). For the modal con-

siderations below the bulk composition of each sample was obtained from XRF analysis of the major elements and the modal composition was obtained from point counting in a thin section of the same sample (see STÜWE and POWELL 1994 and Table 1). Details of the petrography of each sample will be disussed below. The quoted percentages refer to mole-percent normalised to one oxide.

2.1 The Plattengneis samples

Sample 48/92 is a Plattengneis sample from a quarry near Stainz at one of the eastern-most exposures of the Plattengneis. The sample is very similar to many of the samples described in detail by KROHE 1987 and the interested reader is referred there for structural discussion. With 66%, quartz forms the most abundant phase in the sample. 5% muscovite form a strong mylonitic foliation and about 1% of muscovite is late and overgrows the foliation. Garnet forms 9% of the sample. Garnet occurs partly within the foliation as deformed elongated masses of former porphyroblasts but recrystallisation of garnet outlasted deformation and small euhedral phenocrysts overgrow the fabric. 19% biotite occur in the sample. This biotite grows only in pressure shadows around garnet and it appears therefore that it was only stabilised during the deformation from a previously biotite-absent assemblage. A second generation of biotite overgrows statically the fabric of the rock and grows as coronas on muscovite. No good average *PT* estimates were obtained by attempting to use biotite, muscovite and garnet end members which confirms the optically derived interpretation that biotite and muscovite grew or recrystallised during different stages of the evolution of the sample.

Sample 26/92 is from about one kilometre east of the Koralm summit. It was sampled within what is mapped as "Plattengneis" by BECK–MANAGETTA 1980a but the sample is not as intensely deformed as sample 48/92 and comes out of the transition zone in the footwall of the Plattengneis shear zone. With 53% quartz is again the most abundant phase. 13% garnet are present and abundant late muscovite overgrows a foliation which is also formed by muscovite and some biotite. In total there is 22% muscovite and 13% biotite. Similar to sample 48/92, biotite grows only in pressure shaddows around garnet and some late overgrowths on crosscutting muscovite so that it appears to have been stabilised only during and after the deformation. An average *PT* estimate indicates equilibration conditions around 700°C to 720°C and 13.6 to 14 kbar. Interpretation of the formation conditions of this sample on modal grounds is difficult because the abundant late growth of micas has changed the relative proportions of all minerals in the sample.

2.2 The Paramorphoseschiefer sample

Sample 24/92 is a kyanite-rich sample out of the Paramorphoseschiefer from a position which is stratigraphically about 500 m below the Plattengneis near the Koralm summit. It is the only sample in which quartz is one of the less abundant phases (16%). 60% kyanite is the most abundant phase and crystals are very large so that the mode counted in thin section 24/92 may not be representative of the bulk composition. The kyanite forms fine-grained paramorphs after large andalusite porphyroblasts. The foliation is less-pronounced than in the two samples discussed above, but is defined by about 9% biotite and 10% muscovite. 5% garnet occurs as dispersed small porphyroblasts. Retrograde reaction of kyanite with garnet forms muscovite seams between the two minerals. Tourmaline occurs in the sample as the most abundant accessoric phase. Average *PT* estimates for this sample indicate equilibration conditions of about 630°C and 13.4 kbar.

2.3 The Zentraler Gneis Komplex sample

Sample 29/92 is from a locality in the Friesachgraben from an elevation of 1000m above sea level on the western slope of the Koralm. The sample contains 35% quartz, 20% biotite, 27% muscovite and 15% garnet and is the least-deformed sample. This particular sample was selected because garnets can be observed to react to very fine-grained sillimanite which has previously not been reported from the Koralm crystalline complex. Garnets appear well-equilibrated. Because of the lack of an intense fabric it cannot be clearly established how much of the micas grew postdate to the deformation history. The sample is therefore exceptional with respect to its record of high T at relatively low P that this paragenesis records (see below). Average PT estimates had very large error limits but indicated exceptionally high temperatures around 750°C at 13–14 kbar which is consistent with the occurrence of retrograde sillimanite.

3. Thermodynamic pseudosections

This section introduces four thermodynamic pseudosections calculated for the bulk compositions discussed above (Table 1). The pseudosections were calculated with the software package THERMOCALC of Powell and Holland 1989 and the thermodynamic dataset of Holland and Powell 1990 in the PT range of 3.5–20 kbar and 550°C–750°C. Details of the method of calculation are summarised by Xu et al 1994 and Stüwe and Powell 1994. In order to make the information of these diagrams accessible to as wide of an audience as possible, it is preceded by a brief review of the definition of pseudosections and how to read them.

Figure 1.: (a) A theoretical petrogenetic grid containing only one univariant reaction between phases A, B, C and D in a ternary system. (b) A pseudosection of this grid for a bulk composition shown by the white circle in the compatibility diagrams shown in (c). In the compatibility diagrams white fields are divariant fields, shaded fields indicate tieline bundles in trivariant fields, black areas indicate quadrivariant one-phase stability fields.

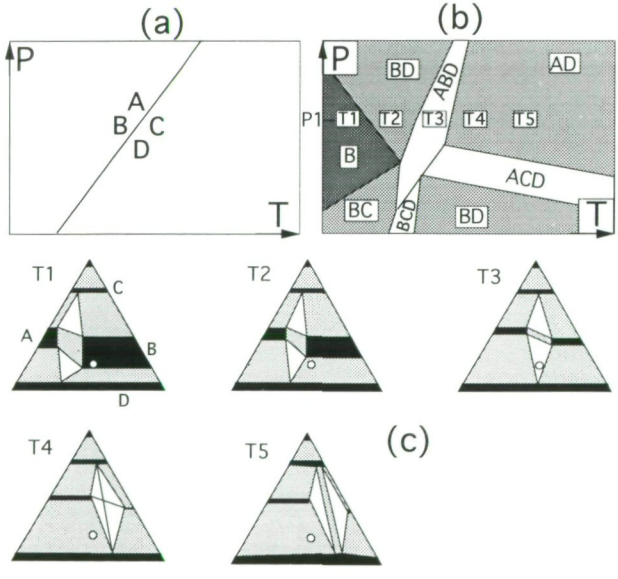

3.1 What are pseudosections ? — a refresher

Pseudosections are partial petrogenetic grids, for example *PT*-grids, that show only those reactions and reaction fields that are of relevance to a given bulk composition. As an example, consider a univariant reaction between four hypothetical phases A, B, C and D in a ternary (3 component) system (*uni* variant because of *one* degree of freedom, as derived from phase rule: #Phases = #Components - #Freedom + 2). The petrogenetic grid for this reaction is shown in Figure 1a. This univariant reaction is the locus of all points in *PT* where the tieline between phases A and B in the ternary compatibility diagram breaks down to a tieline between C and D but it is important to note that *no* real bulk compositions (except the one that is located exactly at the crosspoint of the tie lines) will evidence the net effect of the reaction as being A+B->C+D. Instead, real bulk compositions will record any of the four reactions A+B+C->C+D+A; A+B+D->C+D+A; A+B+C->C+D+B or A+B+D->C+D+B which is the consequence of forming one divariant assemblage from another by crossing the univariant reaction. This can only be shown on a pseudosection. In fact, many bulk compositions that do not have a divariant assemblage near the *P* and *T* where the reaction is crossed will not "see" the univariant reaction at all. In this case, the univariant reaction is not shown at all on the pseudosection. For an illustration, consider Figure 1b and 1c. Figure 1b is a pseudosection of Figure 1a for the bulk composition shown by the white circle in the compatibility diagrams of Figure 1c. At a chosen pressure of P1 and temperature T1 the bulk composition is inside the stability field of phase B (Figure 1c) and the assemblage is therefore made up of only this one phase (Figure 1b). It is quadrivariant in the ternary system considered. At T2 the equilibrium compositions of the phases have shifted so that the bulk composition is now within a two-phase field B+D. It is trivariant. Further temperature increase may shift the divariant field A+B+C over the bulk composition so that A will appear in it as a third phase. The assemblage is now divariant. At temperature T4 the univariant reaction A+B->C+D occurs. However, by then the equilibria have shifted so far to the right side of the diagram that the bulk composition has reached again trivariance in the two-phase field A+D so that it does not experience the univariant reaction. The univariant does therefore not appear on Figure 1b at the pressure P1. Further temperature increase to T4 will stabilise now the tieline C+D but will not cause any further changes to the trivariant assemblage of our bulk composition. Just as only part of the reaction of interest appears on Figure 1b, many other univariants that may occur on the full petrogenetic grid may not appear at all on a corresponding pseudosection.

The theoretical reaction illustrated in Figure 1 is actually similar to the staurolite isograde with the phases involved being largely equivalent to A = garnet, B = chlorite, C = staurolite and D = biotite. The positions of the phases in the compatibility diagrams correspond, at least topologically correctly, to those in the part of the AFM projection with muscovite, quartz and fluid in excess.

3.2 Pseudosections of the four samples

Figure 2a–h shows four pseudosections calculated in the model system KFMASH for the bulk compositions of the selected samples (Table 1) in the *T* range of 540°C–750°C. For readability each pseudosection is divided into two parts, a low pressure part from 3.5–14 kbar (Figure 2a–d) and a high pressure part from 9–20 kbar (Figure 2e–h). The low pressure parts show the di- tri- and quadrivariant fields, the high pressure parts also show the modal proportions of minerals in each of the fields. These modal proportions are given in mole-percent normalised to one oxide so that the contour value has to be multiplied by the molar volume and divided by the number of oxides

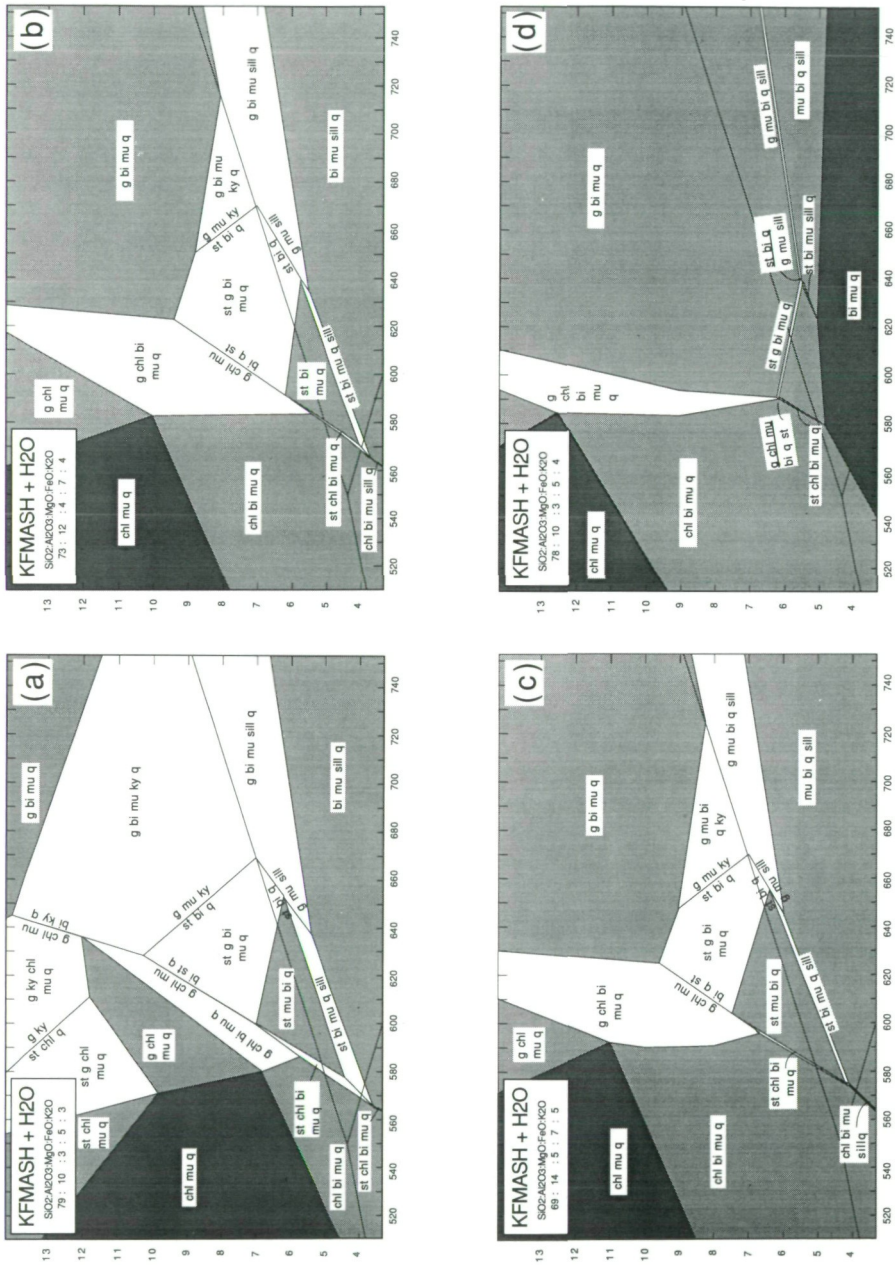

Figure 2: Pseudosections of the four samples discussed here in the *PT* range between 540°C and 750°C and 3.5 kbar to 20 kbar. The pseudosections were calculated with the software package THERMOCALC in the model system KFMASH. Divariant fields are white, trivariant fields are light-shaded, quadrivariant fields are dark-shaded. Figure 2a–d show the low-*P* part of pseudosection for samples 24/92 (Fig.2a); 26/92 (Fig.2b); 29/92 (Fig.2c) and 48/92 (Fig.2d).

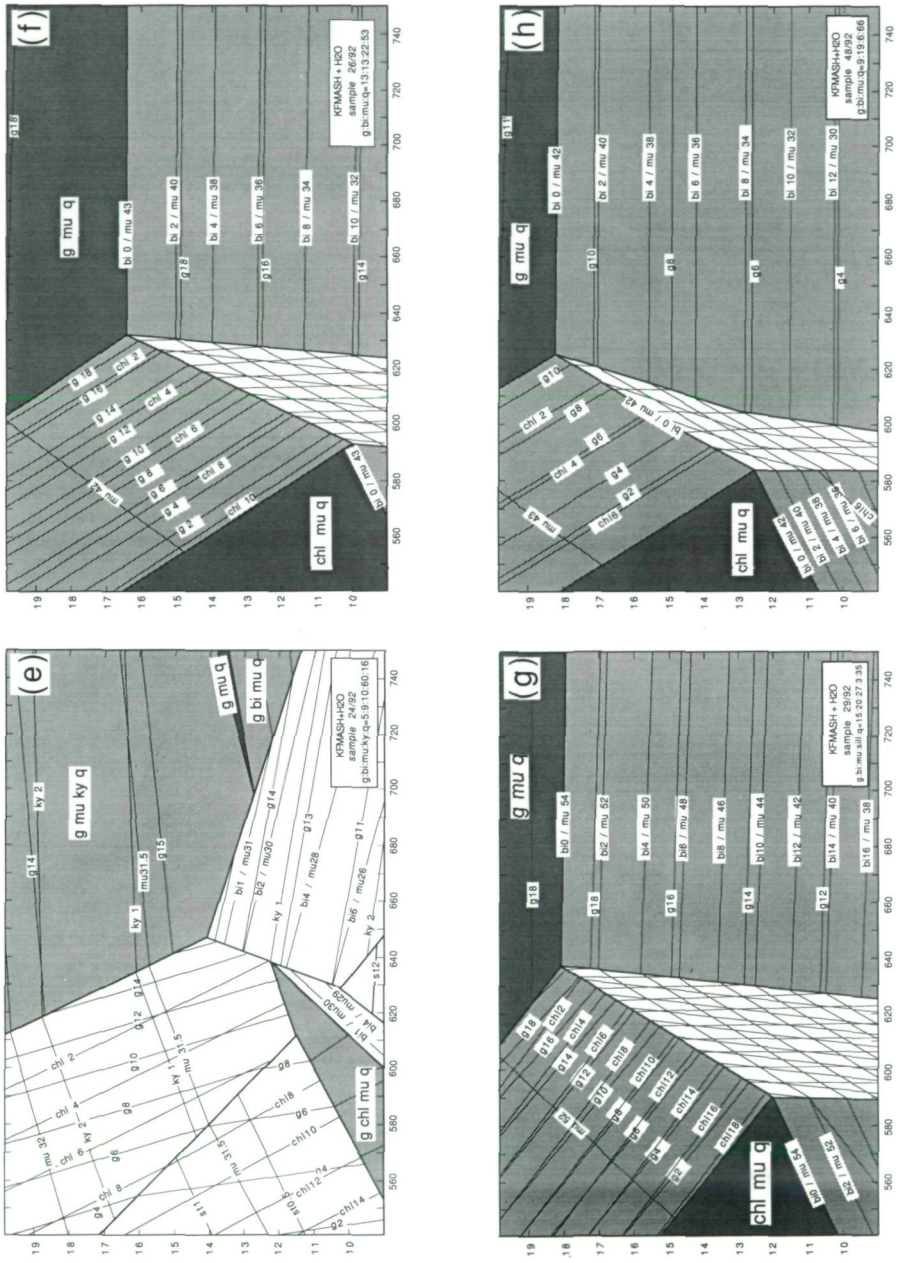

Figures 2e–h show the high-*P* part of the same pseudosections: 24/92 (Fig.2e); 26/92 (Fig.2f); 29/92 (Fig.2g) and 48/92 (Fig.2h). Modal proportions of minerals shown in Fig.2e–h are given in mole percent normalised to one oxide.

(a)

Sa#	Rock Type	ΣKFMASH	K : F : M :A : S
24/92:	Biotite Mica Schist	91.91	3 : 5 : 3 : 10 : 79
26/92:	PG Koralmsumit	93.56	4 : 7 : 4 : 12 : 73
29/92:	Biotite Mica Schist	92.63	5 : 7 : 5 : 14 : 69
48/92:	PG Stainz	93.39	4 : 5 : 3 : 10 : 78

(b)

Sa#	g	bi	mu	sill	ky	q	total
24/92	5	9	10	---	60	16	100%
26/92	13	13	21	---	---	53	100%
29/92	15	20	27	3	---	35	100%
48/92	9	19	6	---	---	66	100%

Table 1: Bulk and modal composition of the four samples selected for this study (after STÜWE and POWELL, 1994). The bulk composition (a) are given for the KFMASH components of an XRF analysis normalised to 100%. The modal composition (b) are given in mole percent normalised to one oxide. For full details of the XRF data and point counting results see Stüwe and Powell, (1994).

in one formula unit to give the volumetric proportion of the mineral in the rock. All further discussion assumes the assemblages to be stable in the presence of water and the mineral abbreviations used correspond to those used by XU et al. 1994 and STÜWE and POWELL 1994. The pseudosections may be compared with the full petrogenetic grid from which these sections are derived as published by XU et al. 1994. In contrast to the full petrogenetic grid, only small parts of very few univariant reactions appear on the pseudosections. These are the reactions

st + bi + q = g + mu + sill		(on: 24/92; 26/92; 29/92; 48/92)
g + chl + mu = bi + st + q	(st-isograde)	(on: 24/92; 26/92; 29/92; 48/92)
st + bi + q = g + mu + ky		(on: 24/92; 26/92; 29/92)
st + chl + mu = bi + sill + q		(on: 24/92; 26/92; 29/92)
g + chl + mu = bi + ky + q		(on: 24/92)
st + chl = g + ky + q	(degenerate)	(on: 24/92)

In most of the high-pressure parts of the pseudosections no univariant reactions appear at all. The di- tri- and quadrivariant reaction fields appearing on the pseudosections are:

divariant reactions

g + chl + bi + mu + q	(on: 24/92; 26/92; 29/92; 48/92)
st + g + bi + mu + q	(on: 24/92; 26/92; 29/92; 48/92)
g + bi + mu + sill + q	(on: 24/92; 26/92; 29/92; 48/92)
st + bi + mu + sill + q	(on: 24/92; 26/92; 29/92; 48/92)
st + chl + bi + mu + q	(on: 24/92; 26/92; 29/92; 48/92)
g + bi + mu + ky + q	(on: 24/92; 26/92; 29/92)
chl + bi + mu + sill + q	(on: 26/92; 29/92)
st + g + chl + mu + q	(on: 24/92)
g + chl + mu + ky + q	(on: 24/92)

trivariant reactions

g + chl + mu + q	(on: 24/92; 26/92; 29/92; 48/92)
chl + bi + mu + q	(on: 24/92; 26/92; 29/92; 48/92)
g + bi + mu + q	(on: 24/92; 26/92; 29/92; 48/92)
st + bi + mu + q	(on: 24/92; 26/92; 29/92; 48/92)
bi + mu + sill + q	(on: 24/92; 26/92; 29/92; 48/92)
g + mu + ky + q	(on: 24/92)
st + chl + mu + q	(on: 24/92)

quadrivariant reactions

g + mu + q	(on: 24/92; 26/92; 29/92; 48/92)
chl + mu + q	(on: 24/92; 26/92; 29/92; 48/92)
bi + mu + q	(on: 48/92)

It is interesting to compare their topological similarity of the four pseudosections with the similarity of the bulk compositions (Table 1). The pseudosections for sample 26/92 and 29/92 are topologically identical with the only difference being the *PT* conditions of the first divariant appearance of garnet which are somewhat higher fore sample 29/92. In sample 48/92 the same divariant fields occur but they are much narrower and some of the low-*P* assemblages have made room for the quadrivariant assemblage bi-mu-q. Both is a consequence of the low Al content of the sample. Indeed, the assemblage bi-mu-q is a common quadrivariant assemblage for many Al-poor rocks of the Austroalpine at lower grades. The pseudosection for sample 24/92 is similar to the other three at low and intermediate *P* up to about 9 kbar but substantially different at higher *P*. The difference is evidenced by the appearance of ky-bearing divariant assemblages equivalent to the trivariant assemblages in the other pseudosections. The appearance of ky in this pseudosection is because of the high Al/(Fe+Mg) ratio of the sample although the overall Al-content is low compared to the other samples. Moreover, the K_2O content of this sample is low so that the possibility of using Al to form micas is limited.

4. Geological interpretation and discussion

Whilst it is not the purpose of this paper to preempty conclusions on the *PT* evolution of the rocks for which the pseudosections were calculated, this section summarises a few general remarks on the interpretation of the pseudosections of Figure 2. The divariant fields appearing on all pseudosections are consistent with the geological evidence inasmuch as they show common assemblages in pelitic gneisses of the Austroalpine. This concerns particularly the assemblages g+chl+bi+mu+q, g+bi+mu+q, chl+bi+mu+q, g+chl+mu+q and chl+mu+q and, at high *P*, the quadrivariant assemblage g+mu+q. Indeed, a very large number of rocks in the Austroalpine contain the assemblage g+bi+mu+q±ky which is, depending on the presence of the alumosilicate, either di- or trivariant (with H_2O in excess) and covers a large *PT* region above about 600°C and above 7–8 kbar. This assemblage finds its upper *T* limit only in the muscovite breakdown to potassium feldspar at about 800°C and its upper *P* limit about 16 kbar where biotite disappears out of the assemblage. All four samples discussed here have this assemblage, which is consistent with thermobarometric estimates for the samples. While this pseudosection information is much more detailed than what can be read from the full petrogenetic grid, the trivariant fields cover a large region of *PT* space and where*within* this field the assemblages equilibrated can only be determined with careful thermobarometry or with the aid of the modal proportion contours in Figure 2e–h. In all four sections, the modal amounts of garnet, which is the only phase that did not continue to grow during the retrograde evolution, correspond to forma-

tion around 16 kbar and above 620°C. This is consistent with thermobarometric estimates of STÜWE and POWELL 1994 and EHLERS et al. 1994 who suggest similar pressures and peak temperatures around 700°C. A high pressure pre-history in the quadrivariant field g-mu-q may be inferred from the appearance of biotite only during the deformation. Isobaric cooling from the peak is inferred for some samples because of the late stage muscovite growth which would not be possible if decompression would have continued within the trivariant field g-bi-mu-q (Figure 2h). Reequilibration on the retrograde path at much lower *P* is indicated in sample 29/92 from pervasive mica growth (Figure 2c, g). The presence of retrograde sillimanite indicates that it must have crossed the divariant field g+bi+mu+sill+q on the retrograde path (Figure 2c) which is only possible if temperatures were still above 650°C at 7 kbar. In sample 26/92 biotite appears only during deformation and it too appears to indicate decompression from the quadrivariant assemblage g+mu+q into the trivariant field g+bi+mu+q (Figure 2b,f). In sample 24/92 biotite is also usually late, indicating decompression and cooling from the trivariant assemblage g+mu+ky+q into the divariant field g+bi+mu+ky+q (Figure 2a, e). Retrograde staurolite is absent from all samples studied here implying that temperatures at 7–8 kbar were either above 660°C or below 590°C.

5. Conclusions

Pseudosections that are calculated for common pelitic bulk compositions of the Koralm crystalline complex within the model system KFMASH, show di- tri- and quadrivariant fields that are consistent with assemblages commonly observed in these rocks. Of particular interest for the Koralm complex are the trivariant reaction fields g+bi+mu+q+H_2O, chl+bi+mu+q+H_2O, g+ky+mu+q+H_2O and g+chl+mu+q+H_2O as well as the divariant fields g+chl+bi+mu+q+H_2O, g+ky+bi+mu+q+H_2O and st+g+bi+mu+q+H_2O. The common trivariant assemblage g+bi+mu+q+H_2O is shown to be stable in the *PT* range between about 600°C and 800°C and 7–18 kbar. This information is more detailed than what can be read from the full petrogenetic grid, but further constraints can be obtained from modal proportion contours of minerals within this field. For the Plattengneis these indicate an early high-*P* history, equilibration at 700°C and about 14–16 kbar and initial isobaric cooling after the Eoalpine temperature peak. For other rocks more detailed constraints are less clear but the presence of retrograde sillimanite in at least one sample indicates still high temperatures at comparably low pressures.

Acknowledgements

R. POWELL, G. XU, and T.J.B. HOLLAND are thanked for a number of discussions about the calculation of pseudosections. W. FRANK is thanked for a number of days in the field. K. EHLERS and E. PAUL are thanked for revisions of earlier versions of this manuscript.

References

BECK-MANAGETTA, P. (1980a): Geologische Karte der Republik Österreich 1:50.000, Nr. 188 Wolfsberg – Geol. B.-A., Wien.

BECK-MANAGETTA, P. (1980b): Die Koralpe. In: Der geologische Aufbau Österreichs. Geol. B.-A. Wien, 386–392.

CHAMBERLAIN, P. (1986): Evidence for the repeated folding of isotherms during regional metamorphism. – J.Pet. 27: 63–89.

EHLERS, K., STÜWE, K., POWELL, R., SANDIFORD, M. & FRANK, W. (1994): Thermometrically inferred cooling rates of the Koralm crystalline complex, eastern Alps, Austria. Evidence for shear heating ? – Earth.Plan.Sci.Let. 125: 307–321.

FRANK, W., ESTERLUS, M., FREY, I., KROHE, A. & WEBER, J. (1983): Der relative Ablauf der Metamorphosegeschichte von Stub- und Koralmkristallin und die Beziehung zum Grazer Paläozoikum. – Jber.Hochschulschwerpunkt S15, 4: 229–236.

HERITSCH, H. (1978): Die Metamorphose des Schiefergneis-Glimmerschiefer-Komplexes der Koralpe, Steiermark. – Mitt.naturwiss.Ver.Steiermark 108: 19–30.

HOLLAND, T.J.B. & POWELL R. (1990): An enlarged and updated internally consistent thermodynamic dataset with uncertainties and correlations: the system K2O-Na2O-CaO-MgO-MnO-FeO-Fe2O3-Al2O3-TiO2-SiO2-C-H2-O2. – J. Met. Geol. 8: 89–124.

KLEINSCHMIDT, G., ENGEL, S., KUNDRUS, K.V. & WOLF, D. (1984): Bericht 1980 über geologische Aufnahmen im Kristallin der südlichen Koralpe auf Blatt 205 St.Paul i.L. – Verh.Geol. B.-A. 1981: A116–120.

KROHE, A. (1987): Kinematics of Cretaceous nappe tectonics in the Austroalpine basement of the Koralm region (eastern Austria). – Tectonophys 136: 171–196.

MILLER, C. (1990): Petrology of the type locality eclogites from the Koralpe and Saualpe (Eastern Alps), Austria. – Schweiz.Min.Pet.Mitt. 70: 287–300.

MORAUF, W. (1982): Rb-Sr und K-Ar Evidenz für eine intensive alpidische Beeinflussung der Paragesteine in Kor- und Saualpe. – Tschermaks Min.Pet.Mitt. 29: 255–282.

POWELL, R. & HOLLAND, T.J.B. (1989): An internally consistent thermodynamic dataset with uncertainties and correlations: 3 application to geobarometry worked examples and a computer program. – J.Met.Geol. 6: 173–204.

SCHNEIDERMAN, J.S. (1990): Use of reaction space in depicting polymetamorphic histories. – Geology 18: 350–353.

STÜWE, K. (1991): Vorläufige Bemerkungen zum möglichen Einfluß der Deformationsgeometrie der Mantlelithosphäre auf die Entwicklung der Ostalpen seit der Kreide. – Mitt.Österr.Geol.Ges.,84: 65–75.

STÜWE, K. & SANDIFORD, M. (1994): Lateral extrusion of the eastern Alps. The role of the mantle lithosphere. – Tectonophys (in press).

STÜWE, K. & POWELL, R. (1994): PT paths from modal proportions. Application to the Koralm complex, eastern Alps – Contributions to Mineralogy and Petrology, in press.

STÜWE, K. & EHLERS, K. (1994): Thermal modelling of the heat budget of the Koralm crystalline complex. Evidence for a transient heat source during the Eoalpine evolution (in prep).

THÖNI, M. & JAGOUTZ, E. (1992): Some new aspects of dating eclogites in orogenic belts: Sm-Nd, Rb-Sr, and Pb-Pb isotopic results from the Austroalpine Saualpe and Koralpe type locality Carinthia/Styria, southeastern Austria. – Geochim. Cosmochim.Acta 56: 347–368.

XU, G., WILL, T. & POWELL, R. (1994): A calculated petrogenetic grid for the system K2O-FeO-MgO-Al2O3-SiO2-H2O, with particular reference to contactmetamorphosed pelites. – J.Met.Geol. 12: 99–119.

Adress: Kurt STÜWE Department of Geology and Geophysics,
The University of Adelaide, Adelaide, SA 5005, Australia.
email: kstuwe@jaeger.geology.adelaide.edu.au.